Introduction

Almost all malignant solid tumors include hypoxic cells due to both excessive consumption and insufficient supply of oxygen within the tumor. Intratumoral hypoxia induces various biological characteristics in tumors. For instance, hypoxia in tumor activates the hypoxia-responsive elements such as hypoxia-inducible factors (HIFs), leading to transcription of target genes including vascular endothelial growth factor (VEGF). VEGF induces angiogenesis, and is also closely related to the proliferation and invasion of tumor. Gene instability caused by hypoxia must affect the differentiation of tumor cells. Intratumoral hypoxic conditions are disadvantageous in term of the production of peroxide radicals, which induces DNA damage under irradiation. Cancer stem cells existing within hypoxic tumor tissue have also been considered to represent a likely cause of radioresistance [1–3]. In glioblastoma, hypoxic conditions play a key role in the development of tumor characteristics. Neuroimaging enabling minimally invasive, objective, and quantitative evaluation of hypoxic conditions in glioblastoma would offer many clinical benefits in terms of diagnosis, selection of treatment, and prediction of prognosis.

Positron emission tomography (PET) using hypoxic cell tracers offers an attractive method for detecting hypoxic cells because it is simple, low-invasive, repeatable, and not limited in applicability to superficial tumors [4]. So far, hypoxic cells in brain tumors have been detected using PET with hypoxic cell tracers such as [^{18}F]fluoromisonidazole (^{18}F-FMISO) [5–7], 1-α-D-(5-deoxy-5-[^{18}F]-fluoroarabinofuranosyl)-2-nitroimidazole (^{18}F-FAZA) [8], and ^{64}Cu-diacetyl-bis(N4-methylthiosemicarbazone) (Cu-ATSM) [9, 10]. A new hypoxic cell tracer, 1-(2-[^{18}F]fluoro-1-[hydroxymethyl]ethoxy)methyl-2-nitroimidazole (^{18}F-FRP170), has recently been identified [11, 12]. PET using ^{18}F-FRP170 (^{18}F-FRP170 PET) has already been performed for detecting hypoxic cells in malignant brain tumors, and the potential of this new tracer has been documented [13]. Several studies assessing intratumoral oxygen condition using electrodes or other methods have confirmed reliability of PET with various hypoxic cell tracers other than ^{18}F-FRP170 [14–17]. However, whether areas of high accumulation on ^{18}F-FRP170 PET really represent tissues including hypoxic cells, and to what degree areas of high accumulation represent regions under hypoxic conditions have remained unclear. The aim of this study was to confirm the reliability of ^{18}F-FRP170 PET for detecting hypoxic cells. We therefore compared standardized uptake value (SUV) measured on ^{18}F-FRP170 PET with intratumoral oxygen pressure (tpO_2) within glioblastoma measured using oxygen microelectrodes during tumor resection. Furthermore, we performed immunohistochemical detection HIF-1, a heterodimeric nuclear transcription factor playing a critical role in cellular response to low oxygen pressure [18], in tissues corresponding to the regions of interest (ROIs) on ^{18}F-FRP170 PET images.

Materials and Methods

Patients

All study protocols were approved by the Ethics Committee of Iwate Medical University, Morioka, Japan (No. H22-70). Patients recruited to this study were admitted to Iwate Medical University Hospital between April 2008 and December 2012. Entry criteria for the study were: patients ≥20 years old with non-treated glioblastoma localized in cerebral white matter other than the brain stem or cerebellum, performance of ^{18}F-FRP170 PET and measurement of absolute oxygen pressure within the tumor according to the study protocol, and voluntary provision of written informed consent to participate. Preoperative diagnosis was based on present history and findings from conventional magnetic resonance imaging (MRI) on admission, and final diagnosis of glioblastoma was made based on histological features after surgery. Twelve patients (ten men, two women, mean age, 63±13.7 years) were enrolled after excluding patients who did not meet the entry criteria (Table 1).

^{18}F-FRP170 PET

Within 7 days (mean, 4.3±2.4 days) before surgery for tumor resection, both conventional MRI including gadolinium-enhanced T1-weighted imaging (Gd-T1WI) and ^{18}F-FRP170 PET were performed. The ^{18}F-FRP170 was synthesized using on-column alkaline hydrolysis according to the methods described by Ishikawa et al. [12]. The final formulation for injection was formed in normal saline containing 2.5 %*v/v* ethanol using solid-phase extraction techniques. At 60 min after intravenous injection of approximately 370 MBq (mean, 5.9±1.8 MBq/kg) of ^{18}F-FRP170, PET was performed using a PET/computed tomography (CT) system (SET3000 GCT/M; Shimazu, Japan). On ^{18}F-FRP170 PET, ROIs of 10 mm in diameter were placed at areas of high accumulation (high-uptake area) and relatively low accumulation (low-uptake area) within the tumor bulk (Fig. 1a, b). These ROIs were placed at regions as close to the brain surface as possible to allow easy and safe insertion of microelectrodes for measuring oxygen pressure during surgery. A ROI was also placed in apparent normal cerebral white matter of the contralateral side. SUV for each ROI was automatically determined. Although both mean and maximal values of SUV in ROI were measured, we defined the mean value of SUV as "SUV" in this study. The normalized SUV, defined as SUV for each high- or low-uptake area divided by SUV for the apparent normal cerebral white matter of the contralateral hemisphere, was also calculated.

Immediately before surgery for each patient, we created a fusion image that combined a three-dimensional ^{18}F-FRP170 PET image with Gd-T1WI using a surgical navigation system (Stealth Station TRIA plus; Medtronics, Minneapolis, MN) in the operation room. On the fusion image, both high- and low-uptake areas were identified stereotactically for each patient (Fig. 2a–d).

Measurement of Intratumoral Oxygen Pressure During Surgery

Measurement of tpO_2 was performed during surgery for aggressive tumor resection. The tpO_2 level was measured using disposable

Table 1. Patient characteristics and measurement data

No.	Sex	Age (year)	Location	SUV			Normalized SUV		tpO_2 (mmHg)		PaO_2 (mmHg)	HIF-1α staining
				High uptake	Low uptake	ANWM	High uptake	Low uptake	High uptake	Low uptake		
1	M	76	Parietal lobe	0.99	0.54	0.54	1.83	1.00	23	44	157	−
2	M	81	Parietal lobe	2.22	1.39	1.04	2.13	1.34	16	45	128	−
3	M	59	Frontal lobe	1.46	1.16	0.87	1.69	1.33	28	56	176	−
4	F	61	Frontal lobe	1.10	0.87	0.74	1.49	1.18	32	54	145	−
5	M	75	Parietal lobe	1.83	1.11	0.83	2.20	1.34	16	33	143	−
6	F	54	Parietal lobe	1.43	0.82	0.62	2.31	1.32	30	54	134	−
7	M	64	Temporal lobe	1.62	1.00	0.72	2.25	1.39	15	27	158	+
8	M	54	Occipital lobe	1.50	1.01	0.76	1.97	1.33	17	35	120	+
9	M	67	Frontal lobe	1.84	1.46	1.13	1.63	1.29	25	36	132	+
10	M	76	Temporal lobe	1.90	0.92	0.77	2.47	1.19	15	26	124	+
11	M	58	Frontal lobe	1.37	1.25	0.90	1.52	1.39	24	34	137	+
12	M	31	Frontal lobe	1.66	1.11	0.87	1.91	1.28	20	37	148	+

ANWM apparent normal white matter, *tpO2* intratumoral oxygen pressure

Clark-type electrodes (UOE-04TS; Unique Medical, Tokyo, Japan) at the tip of a sensor (Teflon-coated tube; diameter, 0.4 mm; length, 10 mm). Immediately before surgery, electrodes were sterilized by immersion in a solution of 2.25 *w/v*% glutaraldehyde and buffer for 2 h, then washed with sterilized physiological saline solution. The electrode was then connected to a digital oxygen pressure monitor (POG-203; Unique Medical) to calibrate the value of oxygen pressure to 150 mmHg in a sterilized physiological saline solution prior to insertion into the tumor. After craniotomy, we stereotactically inserted a needle-shaped navigating marker of 2 mm in diameter into the center region of the high-uptake area where the ROI had been placed before surgery through the dura mater, while we observed the localization of the tip of the marker in the tumor on the monitor of the surgical navigation system (Fig. 2c, d). After removal of the navigation marker, we immediately inserted the electrode along the same trajectory through the dura mater, with the tip of the electrode placed within tumor tissue of the high-uptake area. A digital monitor was then used to measure tpO_2. We observed tpO_2 value gradually declined from 150 mmHg while rising and falling on the digital monitor, and defined the minimum value as the absolute tpO_2 value at the high-uptake area for each patient. After completely washing and calibrating the value of oxygen pressure to 150 mmHg in a sterilized physiological saline solution, the same procedure described above was performed to measure tpO_2 in the low-uptake area. During measurements of tpO_2, arterial oxygen pressure (PaO_2) was measured using arterial blood obtained from the radial artery. After measuring tpO_2 and removing the electrode, we inserted a needle for biopsy along a trajectory to obtain tumor tissues from the high- and low-uptake areas in six patients. In all cases, the tumor was successfully removed after completing the procedures described above.

HIF-1α Immunohistochemistry

Immunohistochemical staining of HIF-1α was performed on specimens obtained from tumor resection for six patients. From all specimens in both high- and low-uptake areas, paraffin-embedded tissue sections of 3-μm-thickness were collected onto 3-aminoprophyltriethoxylane-coated glass slides. The dewaxed preparations were given microwave pretreatment for 30 min in sodium citrate. The preparations were incubated for 60 min using rabbit anti-HIF-1α monoclonal antibody (clone, H1alpha67; Novus Biologicals, Littleton, CO) at 1:200 dilution. Preparations were incubated using peroxidase-based EnVision kits (Dako Japan, Tokyo, Japan) as the secondary antibody, then immersed in diaminobenzidine/H_2O_2 solution for colored visualization. Finally, preparations were counterstained with hematoxylin.

We observed the staining attitude of HIF-1α in tumor cells for all patients. We also evaluated the HIF-1α staining indices for each high- or low-uptake area for each patient, defined as the percentage of cells showing nuclear staining as determined by counting approximately 1,000 cells under light microscopy (×400 magnification).

Statistical Analyses

In all patients, differences in SUV, normalized SUV, and HIF-1α staining index were compared between high- and low-uptake areas using the Mann–Whitney *U* test. Differences in intratumoral pO_2 between high- and low-uptake areas were also compared in all patients using the Mann–Whitney *U* test. Correlations between PaO_2 and tpO_2 and between normalized SUV and tpO_2 for all patients were analyzed in each high- and low-uptake area using Pearson's correlation coefficient test.

Results

Scanning at 60 min after intravenous injection of tracer provided fine contrast images that enabled visual differentiation between high- and low-uptake areas in all patients. In eight patients with glioblastoma presenting a central necrotic region, ^{18}F-FRP170 was partially accumulated in the intermediate layer between the deep layer surrounding the central necrotic region and the outer layer within the peripheral region of tumor involved in lesion enhancement on Gd-T1WI (Fig. 1a, b). Fusion images combining Gd-T1WI and ^{18}F-FRP170 PET provided precise locations of both high- and low-uptake regions during surgery, and allowed us to successfully insert electrodes and obtain the

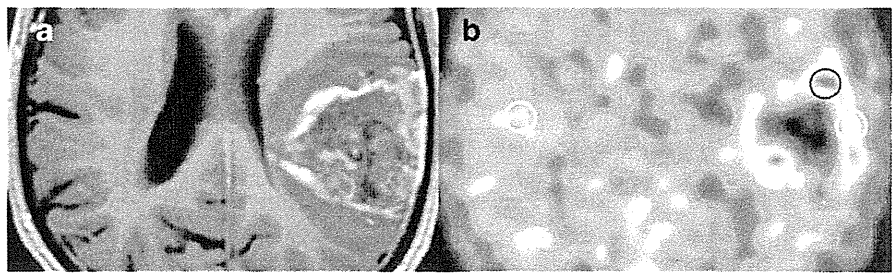

Fig. 1. Typical findings of ^{18}F-FRP170 PET in glioblastoma with a large area of central necrosis in Case 1. High-uptake areas are seen partially in the area between the outer peripheral region showing enhancement on Gd-T1WI and a deeper region adjacent to the central necrotic region. ROIs were placed on a high-uptake area (*black circle*) and a relatively low-uptake area (*white circle*) within the tumor bulk showing enhancement on Gd-T1W, and also on apparent normal white matter of the contralateral hemisphere (*white circle*). **a** Gd-T1WI, **b** ^{18}F-FRP170 PET.

sampling tissues (Fig. 2a–d). No patient presented with any complications due to ^{18}F-FRP170 PET.

Mean SUV for high-uptake areas, low-uptake areas, and contralateral normal white matter regions were 1.58±0.35, 1.05±0.25, and 0.82±0.16, respectively. Significant differences in mean SUV were found between high- and low-uptake areas (p=0.001), between high-uptake areas and normal white matter (p<0.001), and between low-uptake areas and normal white matter (p=0.01), although SUV values in the three groups overlapped (Fig. 3a). Mean normalized SUV for the high- and low-uptake areas were calculated as 1.95±0.33 and 1.28±0.11, respectively. Mean normalized SUV for the high-uptake area differed significantly (p<0.001) and clearly from that of the low-uptake area, with a cut-off level of around 1.4 (Fig. 3b). Mean tpO_2 was significantly lower in high-uptake areas (21.7±

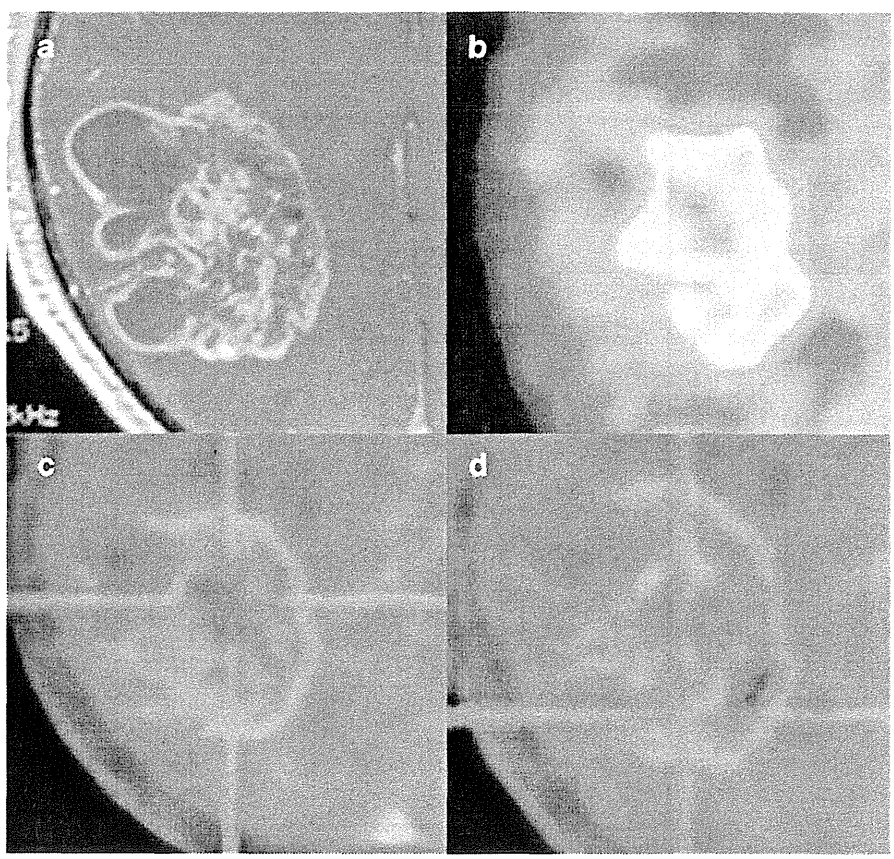

Fig. 2. High- and low-uptake areas were stereotactically localized on fusion images combining Gd-T1WI (**a**) and ^{18}F-FRP170 PET (**b**) for Case 5, to identify tumor tissues corresponding to ROIs. On fusion images, high- and low-uptake areas were depicted as bluish regions (**c**) and greenish regions (**d**), respectively.

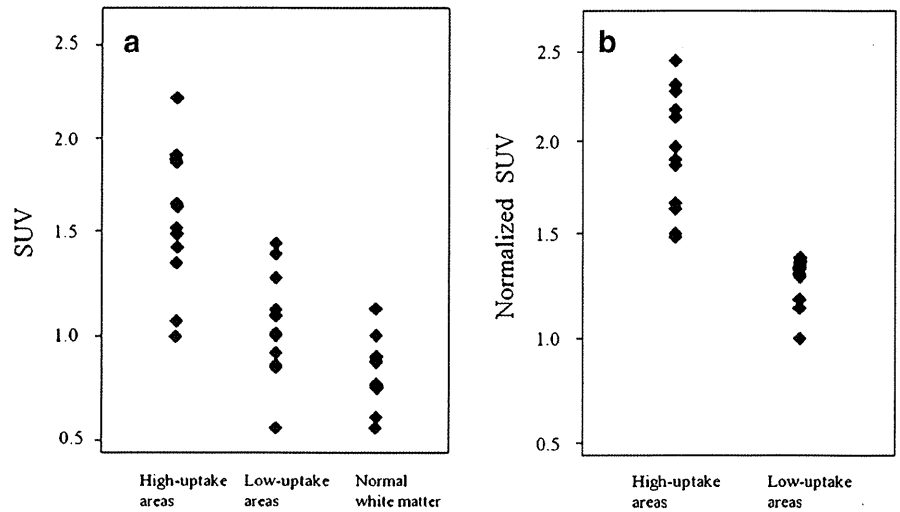

Fig. 3. **a** Differences in SUV among the high-uptake area, low-uptake area, and apparent normal white matter. **b** Difference in normalized SUV between high- and low-uptake areas.

6.2 mmHg) than in low-uptake areas (40.1±10.4 mmHg; $p<0.001$, Fig. 4). In terms of the relationship between normalized SUV and tpO_2 in all patients, a significant negative correlation was found in high-uptake areas ($r=-0.64$, $p=0.03$), whereas no significant correlation was identified in low-uptake areas (Fig. 5a, b). No significant correlations between PaO_2 and tpO_2 were found in either high- or low-uptake areas (not shown).

On specimens obtained from high-uptake areas, HIF-1α was clearly detectable in nuclei in all six patients, with three patients also showing HIF-1α staining in cytoplasm. On the other hand,

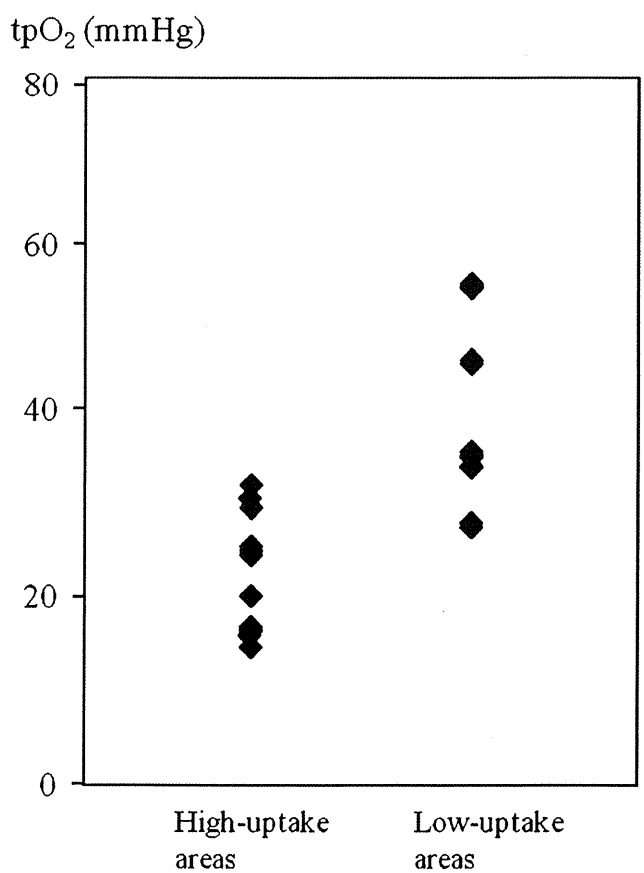

Fig. 4. Difference in tpO_2 between high- and low-uptake areas.

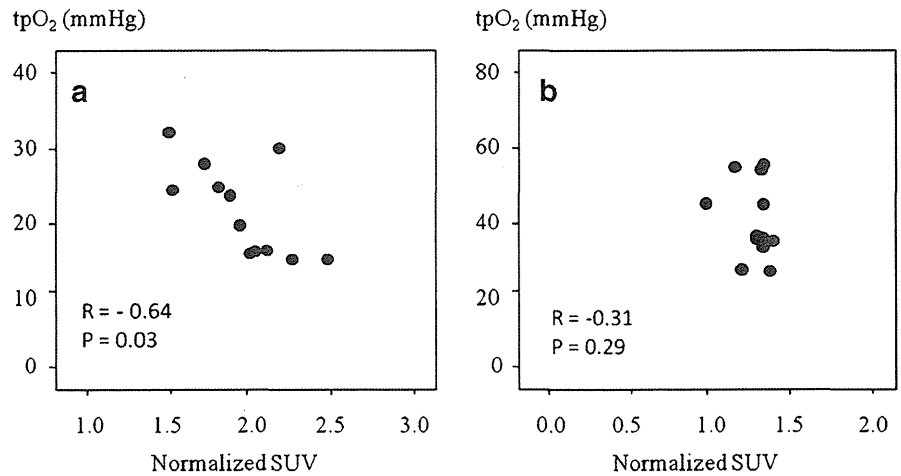

Fig. 5. Correlations between normalized SUV and tpO_2 in high-uptake areas (**a**) and low-uptake areas (**b**).

specimens from low-uptake areas showed three different patterns, with HIF-1α staining only cytoplasm in three patients, and both nuclei and cytoplasm in two patients. In the remaining patient, few barely surviving cells with HIF-1α staining were seen within a wide area of necrotic tissue (Fig. 6a–d). HIF-1α staining indices ranged from 35.2 to 63.5 % in high-uptake areas, and from 8.9 to 35.9 % in low-uptake areas. Mean HIF-1α staining index was significantly higher in high-uptake areas (mean, 53.0±10.2 %) than in low-uptake areas (mean, 18.9± 9.5 %). Notably, HIF-1α staining index was markedly low (8.9 %) in necrotic tissue obtained from a low-uptake area in one patient.

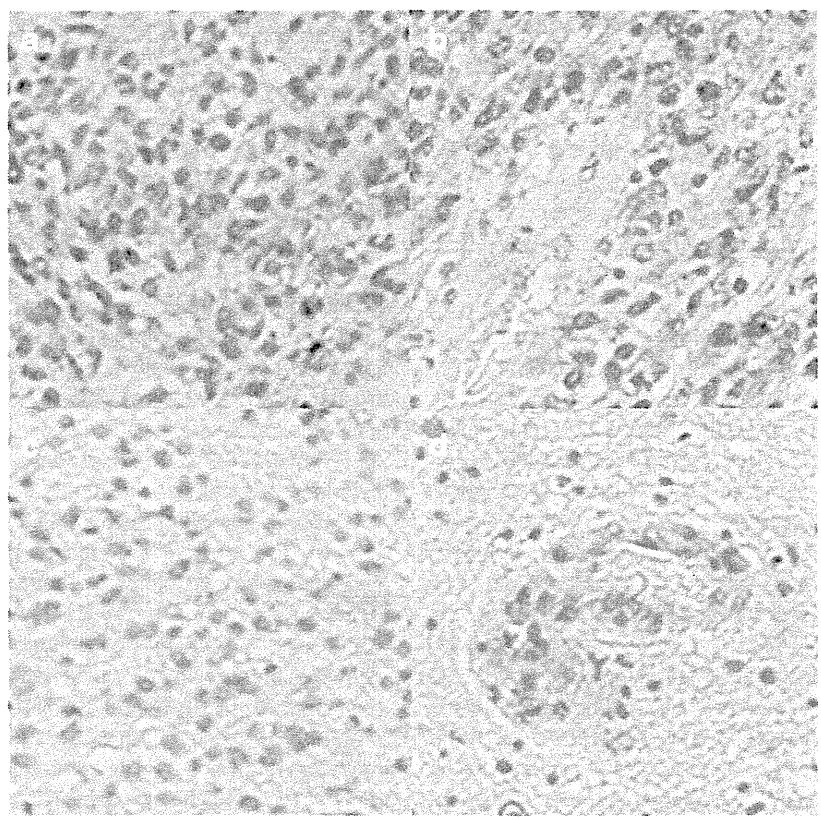

Fig. 6. Findings for HIF-1α immunostaining of tissues from high-uptake areas (**a**, **b**) and low-uptake areas (**c**, **d**). **a** HIF-1α was strongly detected in nuclei in all patients. **b** HIF-1α was stained in both cytoplasms and nuclei in three patients. **c** HIF-1α was stained only in cytoplasm in three patients. **d** A few HIF-1α-stained cells were seen within a wide necrotic tissue in one patient.

Discussion

The present study showed that mean values of both SUV and normalized SUV were significantly higher in high-uptake areas than in low-uptake areas. In particular, normalized SUV values in high-uptake areas were absolutely higher than those in low-uptake areas. In this study, approximately 370 MBq of ^{18}F-FRP170 was administered intravenously for all patients, according to a report by Shibahara et al. [13]. Absolute SUV might thus have been subtly influenced by the delivered volume of tracer into the tumor as determined by individual parameters, such as body size, cardiac output volume, and blood pressure. As normalization of absolute SUV can eliminate differences in these factors, we emphasize the importance of estimation using normalized SUV. In the present study, tpO_2 did not correlate with PaO_2 at all. Two previous reports examining both tpO_2 in brain tumors and PaO_2 could not find any relationship between these measured values, although correlations were not estimated statistically [19, 20]. Our results support those previous reports and indicate that tpO_2 was not influenced by PaO_2 during surgery. Values of tpO_2 were significantly lower in high-uptake areas (21.7± 6.2 mmHg) than in low-uptake areas (40.1±10.4 mmHg). Furthermore, a significant correlation was found between normalized SUV and tpO_2 in high-uptake areas. These results indicate that high-uptake areas where ^{18}F-FRP170 accumulates show relatively more hypoxic conditions than low-uptake areas, suggesting the reliability of findings from ^{18}F-FRP170 PET.

Selective accumulation of ^{8}F-FRP170 in hypoxic cells has been considered to proceed as follows. First, the nitroimidazole moiety in ^{18}F-FRP170 is responsible for the initial accumulation in hypoxic cells. After passive diffusion inside the cells, enzymatic nitroreduction by nitroreductase results in nitroimidazole changing to radical anions. Under normoxic conditions, these radical anions are reoxidized and diffuse out of the cells, whereas products comprising radical anions covalently bound to intracellular macromolecules are trapped within cells under hypoxic conditions [13, 21–23]. As a result, ^{18}F-FRP170 can accumulate only within viable and active hypoxic cells, but cannot accumulate within normoxic cells or even hypoxic cells with low metabolism such as apoptotic or necrotic cells. A previous report assessing accumulation of ^{18}F-FRP170 in a rat model of ischemic myocardium using autoradiography documented that ^{18}F-FRP170 was observed only within viable hypoxic myocardiac cells [11]. As absolute SUV must correlate with the concentration of PET tracer within the tissue, SUV on ^{18}F-FRP170 PET should increase with a higher density of viable hypoxic cells within the tissues of the ROI. We think that such high-uptake areas represent glioblastoma tissue comprising a high density of viable hypoxic cells. In contrast, tissues of low-uptake areas might represent low densities of viable hypoxic cells. In other words, a majority of cells in low-uptake areas could not accumulate ^{18}F-FRP170 because of the presence of either viable cells containing relatively higher tpO_2 than high-uptake area or low metabolic-hypoxic cells degenerating in apoptosis or necrosis. The oxygen environment may thus differ substantially among different regions in low-uptake areas, despite the similar content of viable hypoxic cells. Indeed, tpO_2 levels showed a wide range in low-uptake areas, with a large standard deviation (Fig. 4). This might be one reason for the lack of significant correlation between tpO_2 levels and normalized SUV in low-uptake areas. As intratumoral hypoxia is generally considered to result from insufficient oxygen supply paralleling the distance from normal vessels surrounding the tumor, intratumoral oxygen pressure should be higher in more peripheral regions of glioblastoma that are also supplied with blood from normal vessels surrounding the tumor bulk [24, 25]. On PET in the present study, interestingly, high-uptake areas were observed partially within the intermediate layer of enhancing lesions on Gd-T1WI, and low-uptake areas were seen not only in the peripheral layer external to the intermediate layer containing high-uptake areas but also in the inner core layer adjacent to the central necrosis deep to the intermediate layer (Fig. 1b). We assumed that low-uptake areas in both peripheral and inner core layers might contain little ^{18}F-FRP170-accumulating hypoxic cells, but the peripheral layers included many viable cells at relatively high oxygen pressure, while the inner core comprises low metabolic-hypoxic cells undergoing degenerative apoptosis or necrosis. Remaining low-uptake areas in the intermediate layer probably represent mixture of the two histological types described above. Pistollato et al. [26] evaluated biological characteristics in tissues isolated from three concentric layers (core, intermediate, and peripheral layers) in glioblastoma. The core and intermediate layers showed expression of HIF-1α as a hypoxic cell marker, whereas the peripheral layer did not express HIF-1α, but showed expressions of glial fibrillary acidic protein and β-III-tubulin as mature neural cell markers. In addition, core and intermediate layers contained more glioblastoma stem cells, which are well known to be frequently seen in hypoxic niches. These results suggest that inner core and peripheral layers depicted as low-uptake areas on ^{18}F-FRP170 PET in the present study are likely to exhibit hypoxic and relatively normoxic conditions, respectively.

Hypoxic condition rapidly induces overexpression of HIF-1α for transcripting target genes such as vascular endothelial growth factor to induce angiogenesis, as countermeasures against hypoxic conditions. Under normoxic conditions, prolyl hydroxylation is induced in HIF-1α, allowing binding to the von-Hipple-Lindau protein, which mediates ubiquitination of HIF-1α and subsequent proteasomal degeneration in the cytoplasm. However, under hypoxic conditions, the oxygen requiring prolyl hydroxylase remains inactive, resulting in accumulation of the constitutively expressed HIF-1α protein in cytoplasm. This subunit is phosphorylated and translocated to the nucleus, where it dimerizes with the HIF-1β subunit, binding to the hypoxia-

response elements upstream of HIF-1-regulated target genes [27]. Therefore, increasingly activated-HIF-1α induced by hypoxia accumulates in the nucleus. In this study, all specimens obtained from high-uptake areas clearly showed nuclear staining for HIF-1α, whereas this finding was seen in low-uptake areas in only two patients. Furthermore, mean HIF-1α staining index determined by the percentage of cells showing nuclear staining was significantly higher in high-uptake areas than in low-uptake areas. Necrotic tissue obtained from a low-uptake area of one patient showed an extremely low HIF-1α staining index. These findings might support the concept that high-uptake areas represent more hypoxic regions with a high density of viable and active hypoxic cells. Tissues of low-uptake areas were not obtained from deeper than high-uptake areas but rather from the same depth or more externally during surgery in all six patients. As a result, HIF-1α was also detected in the low-uptake areas of all patients, but showed a greater variety of features than high-uptake areas. These findings support the possibility that low-uptake areas comprised either numerous viable cells under conditions of relatively higher oxygen pressure or low metabolic hypoxic cells under degenerative apoptosis or necrosis.

In the present study, PET at 60 min after intravenous injection of ^{18}F-FRP170 could provide visually fine-contrast PET images. Shidehara et al. [13] reported fine-contrast color images provided by imaging at 120 min after injection of ^{18}F-FRP170 in patients with malignant brain tumor. Kaneta et al. [21] reported that imaging results at 120 min after injection of ^{18}F-FRP170 for patients with lung cancer contributed only a slightly higher tumor/blood ratio when compared with that at 60 min, and concluded that imaging at 60 min after administration was clinically sufficient for assessing hypoxic cells in tumors. The present study supported these recommendations by Kaneta et al. In an experimental study using mice bearing cultured cancer cells, ^{18}F-FAZA displayed significant higher tumor-to-background ratios compared with ^{18}F-FMISO and another azomycin-based nucleoside, iodoazomycin arabinoside, labeled with ^{124}I (^{124}I-IAZA), when scanning for all tracer was fixed in 3 h post-injection [28]. Clinically, PET imaging with ^{18}F-FMISO and ^{18}F-FAZA has usually been scanned at 120–140 [5–7] and 120–210 min [8] after administration, respectively. Although no previous reports have directly compared ^{18}F-FRP170 PET and ^{18}F-FMISO PET images, ^{18}F-FRP170 PET has been considered superior in terms of fine contrast and rapid clearance from blood [21]. The short duration for imaging could represent an additional advantage to ^{18}F-FRP170 PET.

Some limitations regarding the interpretation of study results must be considered for this study. First, the sample size in this study was small. Additional studies of a larger number of patients with glioblastoma are needed. Second, use of smaller ROIs might provide more rigorous results in comparisons among SUV, tpO_2, and histological features. However, in this study, we placed relatively huge ROIs of 10 mm in diameter to avoid misplacement of microelectrodes within the ROI and sampling error of tumor tissues corresponding to the ROI. These issues could represent factors contributing to make maximum SUV within the ROI unsuitable for use in this study. In short, errors involving differences between pinpoint regions for insertion of electrode and maximum SUV could easily anticipated. Third, direct tpO_2 measurements using microelectrodes available differ in sensitivity, accuracy, ability to measure oxygen availability among types of probe used, and impossibility in differentiation between hypoxic and necrotic tissues, although this technique is commonly considered a gold standard [4]. Other techniques indirectly measuring oxygen through reduced drug levels, hemoglobin saturation, or perfusion have been proposed. However, indirect measurements, although valuable, require a set of assumptions to relate the measurement to tpO_2 or oxygen concentration [4]. Fourth, measurement of tpO_2 using electrodes in this study did not strictly represent intracellular oxygen pressure, but rather the oxygen pressure of tissue containing hypoxic cells. However, tpO_2 as measured in this study would correlate with intracellular oxygen pressure, as intracellular oxygen pressure is regulated by extracellular conditions. Fifth, measured tpO_2 values in this study were relatively higher (21.7±6.2 mmHg in high-uptake areas and 40.1±10.4 mmHg in low-uptake areas) than in previous reports of direct measurement using Eppendorf oxygen electrodes in malignant brain tumors, where mean tpO_2 has been reported as approximately ≤20 mmHg [20, 24, 29]. In particular, mean value in low-uptake areas was significantly higher. However, mean tpO_2 in low-uptake areas was lower that of brain tissue around the tumor (59.8±6.5 mmHg) in a previous report [20]. In previous reports regarding oxygen pressure at high-uptake areas on ^{18}F-FMISO PET in animal tumor models, measurements using Eppendorf electrodes showed a high frequency of tpO_2 ≤10 mmHg [15, 30, 31]. Although the reasons for this contradiction are not entirely clear, we consider these results may have arisen from differences in the electrodes used, or from the inflow of a small amount of air into the trajectory when electrodes were inserted immediately after removal of the navigation marker with a larger diameter than the electrode. However, as this issue applied to measurements of tpO_2 for all patients in this study, the findings of higher tpO_2 in high-uptake areas compared to low-uptake areas appear valid.

Conclusions

Findings of a significant correlation between normalized SUV and tpO_2, and strong nuclear immunostaining for HIF-1α in areas of high ^{18}F-FRP170 accumulation, suggest that high-uptake areas on ^{18}F-FRP170 PET represent high densities of viable hypoxic cells, at least in glioblastoma. However, interpretation of low-uptake areas is more complicated, given the likelihood that these lesions comprise

various oxygen environments containing low densities of viable hypoxic cells.

Acknowledgments. This study was supported in part by Grant-in-Aid for Strategic Medical Science Research Center for Advanced Medical Science Research from the Ministry of Science, Education, Sports and Culture, Japan.

Conflict of Interest. The authors declare that they have no conflicts of interest.

References

1. Jensen RL (2009) Brain tumor hypoxia: tumorigenesis, angiogenesis, imaging, pseudoprogression, and as a therapeutic target. J Neurooncol 92:317–335
2. Jensen RL (2006) Hypoxia in the tumorigenesis of gliomas and as a potential target for therapeutic measures. Neurosurg Focus 20:E24
3. Rich JN (2007) Cancer stem cells in radiation resistance. Cancer Res 67:8980–8984
4. Mendichovszky I, Jackson A (2011) Imaging hypoxia in gliomas. Br J Radiol 84(2):S145–S158
5. Eschmann SM, Paulsen F, Reimold M et al (2005) Prognostic impact of hypoxia imaging with 18F-misonidazole PET in non-small cell lung cancer and head and neck cancer before radiotherapy. J Nucl Med 46:253–260
6. Kawai N, Maeda Y, Kudomi N et al (2011) Correlation of biological aggressiveness assessed by 11C-methionine PET and hypoxic burden assessed by 18F-fluoromisonidazole PET in newly diagnosed glioblastoma. Eur J Nucl Med Mol Imaging 38:441–450
7. Swanson KR, Chakraborty G, Wang CH et al (2009) Complementary but distinct roles for MRI and 18F-fluoromisonidazole PET in the assessment of human glioblastomas. J Nucl Med 50:36–44
8. Postema EJ, McEwan AJ, Riauka TA et al (2009) Initial results of hypoxia imaging using 1-alpha-D: -(5-deoxy-5-[^{18}F]-fluoroarabinofuranosyl)-2-nitroimidazole (^{18}F-FAZA). Eur J Nucl Med Mol Imaging 36:1565–1573
9. Sheehan JP, Popp B, Monteith S et al (2011) Trans sodium crocetinate: functional neuroimaging studies in a hypoxic brain tumor. J Neurosurg 115:749–753
10. Tateishi K, Tateishi U, Sato M et al (2013) Application of ^{62}Cu-diacetyl-bis (N4-methylthiosemicarbazone) PET imaging to predict highly malignant tumor grades and hypoxia-inducible factor-1alpha expression in patients with glioma. AJNR Am J Neuroradiol 34:92–99
11. Kaneta T, Takai Y, Kagaya Y et al (2002) Imaging of ischemic but viable myocardium using a new 18F-labeled 2-nitroimidazole analog, 18F–FRP170. J Nucl Med 43:109–116
12. Ishikawa Y, Iwata R, Furumoto S, Takai Y (2005) Automated preparation of hypoxic cell marker [^{18}F]FRP-170 by on-column hydrolysis. Appl Radiat Isot 62:705–710
13. Shibahara I, Kumabe T, Kanamori M et al (2010) Imaging of hypoxic lesions in patients with gliomas by using positron emission tomography with 1-(2-[^{18}F] fluoro-1-[hydroxymethyl]ethoxy)methyl-2-nitroimidazole, a new 18F-labeled 2-nitroimidazole analog. J Neurosurg 113:358–368
14. Matsumoto K, Szajek L, Krishna MC et al (2007) The influence of tumor oxygenation on hypoxia imaging in murine squamous cell carcinoma using [^{64}Cu]Cu-ATSM or [^{18}F]Fluoromisonidazole positron emission tomography. Int J Oncol 30:873–881
15. Sorensen M, Horsman MR, Cumming P et al (2005) Effect of intratumoral heterogeneity in oxygenation status on FMISO PET, autoradiography, and electrode Po2 measurements in murine tumors. Int J Radiat Oncol Biol Phys 62:854–861
16. Mahy P, De Bast M, Gallez B et al (2003) In vivo colocalization of 2-nitroimidazole EF5 fluorescence intensity and electron paramagnetic resonance oximetry in mouse tumors. Radiother Oncol 67:53–61
17. Tran LB, Bol A, Labar D et al (2012) Hypoxia imaging with the nitroimidazole ^{18}F-FAZA PET tracer: a comparison with OxyLite, EPR oximetry and 19F-MRI relaxometry. Radiother Oncol 105:29–35
18. Wang GL, Semenza GL (1995) Purification and characterization of hypoxia-inducible factor 1. J Biol Chem 270:1230–1237
19. Collingridge DR, Piepmeier JM, Rockwell S, Knisely JP (1999) Polarographic measurements of oxygen tension in human glioma and surrounding peritumoural brain tissue. Radiother Oncol 53:127–131
20. Kayama T, Yoshimoto T, Fujimoto S, Sakurai Y (1991) Intratumoral oxygen pressure in malignant brain tumor. J Neurosurg 74:55–59
21. Kaneta T, Takai Y, Iwata R et al (2007) Initial evaluation of dynamic human imaging using ^{18}F-FRP170 as a new PET tracer for imaging hypoxia. Ann Nucl Med 21:101–107
22. Chapman JD (1979) Hypoxic sensitizers—implications for radiation therapy. N Engl J Med 301:1429–1432
23. Krohn KA, Link JM, Mason RP (2008) Molecular imaging of hypoxia. J Nucl Med 49(Suppl 2):129S–148S
24. Beppu T, Kamada K, Yoshida Y et al (2002) Change of oxygen pressure in glioblastoma tissue under various conditions. J Neurooncol 58:47–52
25. Brown JM (1979) Evidence for acutely hypoxic cells in mouse tumours, and a possible mechanism of reoxygenation. Br J Radiol 52:650–656
26. Pistollato F, Abbadi S, Rampazzo E et al (2010) Intratumoral hypoxic gradient drives stem cells distribution and MGMT expression in glioblastoma. Stem Cells 28:851–862
27. Fischer I, Gagner JP, Law M, Newcomb EW, Zagzag D (2005) Angiogenesis in gliomas: biology and molecular pathophysiology. Brain Pathol 15:297–310
28. Reischl G, Dorow DS, Cullinane C et al (2007) Imaging of tumor hypoxia with [^{124}I]IAZA in comparison with [^{18}F]FMISO and [^{18}F]FAZA-first small animal PET results. J Pharm Pharm Sic 10:203–211
29. Rampling R, Cruickshank G, Lewis AD et al (1994) Direct measurement of pO2 distribution and bioreductive enzymes in human malignant brain tumors. Int J Radiat Oncol Biol Phys 29:427–431
30. Piert M, Machulla H, Becker G et al (1999) Introducing fluorine-18 fluoromisonidazole positron emission tomography for the localisation and quantification of pig liver hypoxia. Eur J Nucl Med 26:95–109
31. Bartlett RM, Beattie BJ, Naryanan M et al (2012) Image-guided PO2 probe measurements correlated with parametric images derived from ^{18}F-fluoromisonidazole small-animal PET data in rats. J Nucl Med 53:1608–1615

JJCO Japanese Journal of Clinical Oncology

Original Articles

Jpn J Clin Oncol 2012;42(10)887–895
doi:10.1093/jjco/hys121
Advance Access Publication 27 July 2012

Phase II Study of Single-agent Bevacizumab in Japanese Patients with Recurrent Malignant Glioma†

Motoo Nagane[1,*], Ryo Nishikawa[2], Yoshitaka Narita[3], Hiroyuki Kobayashi[4], Shingo Takano[5], Nobusada Shinoura[6], Tomokazu Aoki[7], Kazuhiko Sugiyama[8], Junichi Kuratsu[9], Yoshihiro Muragaki[10], Yutaka Sawamura[11] and Masao Matsutani[2]

[1]Department of Neurosurgery, Kyorin University Faculty of Medicine, Tokyo, [2]Department of Neuro-Oncology/Neurosurgery, International Medical Center, Saitama Medical University, Saitama, [3]Department of Neurosurgery and Neuro-Oncology, National Cancer Center Hospital, Tokyo, [4]Department of Neurosurgery, Graduate School of Medicine, Hokkaido University, Hokkaido, [5]Department of Neurosurgery, Graduate School of Human Science, University of Tsukuba, Ibaraki, [6]Department of Neurosurgery, Komagome Metropolitan Hospital, Tokyo, [7]Department of Neurosurgery, Kitano Hospital, Osaka, [8]Depatment of Neurosurgery, Hiroshima University School of Medicine, Hiroshima, [9]Department of Neurosurgery, Kumamoto University Faculty of Life Sciences, Kumamoto, [10]Faculty of Advanced Techno-Surgery Graduate School of Medicine, Tokyo Women's Medical University, Tokyo and [11]Sawamura Neurosurgery Clinic, Hokkaido, Japan

*For reprints and all correspondence: Motoo Nagane, Department of Neurosurgery, Kyorin University Faculty of Medicine, 6-20-2 Shinkawa, Mitaka, Tokyo 181-8611, Japan. E-mail: nagane-nsu@umin.ac.jp

†These data were previously presented at the 2011 European Multidisciplinary Cancer Congress, jointly organized by the European CanCer Organisation (ECCO) and European Society for Medical Oncology (ESMO), Stockholm, Sweden, 23–27 September 2011 and the 2011 Society for Neuro-Oncology, CA, USA, 17–20 November 2011.

Received April 18, 2012; accepted July 1, 2012

Objective: This single-arm, open-label, Phase II study evaluated the efficacy and safety of single-agent bevacizumab, a monoclonal antibody against vascular endothelial growth factor, in Japanese patients with recurrent malignant glioma.

Methods: Patients with histologically confirmed, measurable glioblastoma or World Health Organization Grade III glioma, previously treated with temozolomide plus radiotherapy, received 10 mg/kg bevacizumab intravenous infusion every 2 weeks. The primary endpoint was 6-month progression-free survival in the patients with recurrent glioblastoma.

Results: Of the 31 patients enrolled, 29 (93.5%) had glioblastoma and 2 (6.5%) had Grade III glioma. Eleven (35.5%) patients were receiving corticosteroids at baseline; 17 (54.8%) and 14 (45.2%) patients had experienced one or two relapses, respectively. The 6-month progression-free survival rate in the 29 patients with recurrent glioblastoma was 33.9% (90% confidence interval, 19.2–48.5) and the median progression-free survival was 3.3 months. The 1-year survival rate was 34.5% with a median overall survival of 10.5 months. There were eight responders (all partial responses) giving an objective response rate of 27.6%. The disease control rate was 79.3%. Eight of the 11 patients taking corticosteroids at baseline reduced their dose or discontinued corticosteroids during the study. Bevacizumab was well-tolerated and Grade $\geq$3 adverse events of special interest to bevacizumab were as follows: hypertension [3 (9.7%) patients], congestive heart failure [1 (3.2%) patient] and venous thromboembolism [1 (3.2%) patient]. One asymptomatic Grade 1 cerebral hemorrhage was observed, which resolved without treatment.

Conclusion: Single-agent bevacizumab provides clinical benefit for Japanese patients with recurrent glioblastoma.

Key words: bevacizumab – glioblastoma – Asian continental ancestry group – Phase II – glioma

INTRODUCTION

Glioblastoma (GBM) is the most aggressive form of primary malignant brain tumor and the prognosis for patients with GBM is poor (1,2); the majority will relapse following initial treatment and <10% are alive at 5 years (3). The standard treatment for patients with newly diagnosed GBM is surgical resection followed by temozolomide (TMZ) and radiotherapy (RT), and then adjuvant TMZ alone (Stupp regimen) (4). Treatment options for patients with recurrent GBM, however, are limited and include repeat resection, RT and systemic chemotherapy, such as TMZ, nitrosoureas, platinum-based regimens (carboplatin, cisplatin), cyclophosphamide, irinotecan and etoposide, and appropriate treatment will depend on the patient and tumor characteristics (5). Currently there is no standard therapy for recurrent GBM and the estimated 6-month progression-free survival (PFS) rate for patients with recurrent disease is 9–28% (6–11) with a 1-year survival rate of 14–32% (6–8,10,11). Therefore, new treatment strategies for recurrent GBM are needed.

An alternative therapeutic approach is the inhibition of angiogenesis through the vascular endothelial growth factor (VEGF), a key regulator of angiogenesis. High levels of VEGF are expressed in GBM cells (12,13), and hypoxia and acidosis, conditions commonly seen in solid tumors, upregulate VEGF expression in glioma cells *in vivo* (14). In a mouse model, monoclonal antibodies to VEGF have been shown to inhibit the growth of the C6 glioma (15). Bevacizumab (Avastin®) is a monoclonal antibody that inhibits VEGF and is currently approved for a range of metastatic cancers (colorectal, non-small-cell lung, breast, ovarian cancer and renal cancers) (16–19) as well as for use in adults with recurrent GBM in many countries including the USA (20,21). Early Phase II studies in patients with recurrent GBM showed the efficacy of bevacizumab in combination with irinotecan (22,23). Subsequently, two Phase II studies (24–26) showed the efficacy of single-agent bevacizumab with regard to response rates and 6-month PFS in patients with recurrent GBM who had previously received RT and TMZ. These two studies formed the basis of bevacizumab's approval by the Food and Drug Administration (FDA) in 2009. Moreover, other studies have shown the efficacy of bevacizumab in recurrent GBM whether given as a single agent (27) or combined with irinotecan (28,29) and other chemotherapies, such as etoposide, carboplatin and fotemustine (30–33). Given the current evidence for bevacizumab in recurrent GBM in Western patient populations, we investigated the efficacy and safety of single-agent bevacizumab in a Phase II, single-arm, open-label study (JO22506) in Japanese patients with recurrent malignant glioma.

PATIENTS AND METHODS

The trial was carried out in accordance with the principles of Good Clinical Practice and the Declaration of Helsinki; all patients provided written informed consent prior to any study-related procedure. The protocol was approved by the institutional review boards of all participating centers. The study was registered with the Japan Pharmaceutical Information Center-Clinical Trials Information (JapicCTI), trial number: JapicCTI-090841.

Eligibility

Eligible patients were aged ≥20 years with histologically confirmed GBM or World Health Organization (WHO) Grade III glioma, the latter being reconfirmed at the time of surgery for recurrent glioma. Patients had magnetic resonance imaging (MRI)-confirmed disease recurrence or progression with measurable lesions within 2 weeks prior to the first study treatment and no evidence of acute or subacute cerebral hemorrhage and had received prior TMZ and RT for malignant glioma. Other key inclusion criteria were a Karnofsky performance status (KPS) ≥70%, a life expectancy of ≥3 months and adequate hematologic, renal and hepatic function (i.e. absolute neutrophil count ≥1500/mm^3, platelet count ≥100 000/mm^3, hemoglobin ≥10 g/dl, bilirubin ≤ 1.5 × the upper limit of normal (ULN), aspartate aminotransferase and alanine aminotransferase ≤ 2.5 × ULN, serum creatinine ≤ 1.25 × ULN). The following minimum intervals of time must have elapsed between the termination of therapies and the start of bevacizumab treatment: RT 8 weeks; surgical therapy and incisional biopsy 4 weeks; endocrine therapy and immunotherapy 3 weeks; post-traumatic intervention (except for patients with non-healing wounds) 2 weeks; transfusion and the use of hematopoietic growth factors 2 weeks; aspiration cytology and needle biopsy 1 week; nitrosoureas 6 weeks, procarbazine 3 weeks, vincristine 2 weeks and other chemotherapies 4 weeks and other investigational new drugs and unapproved drugs 4 weeks. Patients were excluded if they had: prior treatment with bevacizumab; a history of treatment with carmustine wafers, stereotactic radiotherapy, proton therapy or neutron capture therapy; ≥3 prior regimens for malignant glioma and inadequately controlled hypertension, heart disease, symptomatic cerebrovascular disorder, gastrointestinal (GI) perforation, fistula or abdominal abscess within 6 months prior to enrollment.

Study Design

This single-arm, open-label, Phase II study was conducted at 10 sites in Japan. One cycle of treatment was defined as one

bevacizumab infusion administered on Day 1 every 2 weeks. Eligible patients received 10 mg/kg bevacizumab as an intravenous infusion administered over 90 (± 15) min on Day 1 of each cycle, which could be reduced to 30 min by Cycle 3 if no infusion reactions occurred. Treatment continued until disease progression (PD) or unacceptable toxicity. Bevacizumab doses were adjusted only for changes of ≥10% in body weight during the study. In the event of unacceptable toxicity, bevacizumab treatment was delayed or discontinued according to pre-specified criteria. Bevacizumab was discontinued if multiple adverse events (AEs) fulfilling the pre-specified delay or discontinuation criteria occurred in the same cycle, if cerebral hemorrhage occurred and if delayed treatment could not be restarted within 6 weeks of the last bevacizumab infusion. Patients who discontinued bevacizumab were followed for survival. Bevacizumab was provided by Chugai Pharmaceutical Co. Ltd (Tokyo, Japan).

Assessment of Efficacy

The primary endpoint was 6-month PFS in patients with recurrent GBM only. Six-month PFS was defined as the percentage of patients who remained alive and progression free at 24 weeks and was chosen based on published evidence demonstrating its extrapolation to the overall survival (OS) (6,7). Secondary efficacy endpoints included the 1-year survival, PFS, objective response rate (ORR), duration of response (DOR), OS and disease control rate (DCR).

Efficacy was assessed every third cycle (i.e. Cycles 3, 6, 9 etc.). Progression and objective response were determined by comprehensive evaluation of the results from MRI scans, corticosteroid dose assessment and neurocognitive function assessment. They were assessed by an independent radiology facility (IRF) by reference to Macdonald's Criteria (34). Response was classified according to the following categories: complete response (CR), partial response (PR), no change (NC) and PD. Confirmation of the response was determined on two consecutive assessments ≥4 weeks apart: patients who were determined as having CR or PR were defined as responders; patients who were determined as having NC or PD were defined as non-responders.

Percentage tumor shrinkage was also assessed and was calculated from the sum of the products of the diameters (SPD) at baseline and the smallest SPD after baseline.

Assessment of Safety

AEs were assessed throughout the study and were graded according to the Common Terminology Criteria for AEs version 3.0 (35). Body weight, vital signs and laboratory tests were assessed prior to the start of each cycle.

Statistical Methods

The efficacy analysis population comprised all patients with recurrent GBM. Patients with Grade III glioma were also evaluated for efficacy, but were not included in the primary analysis. All patients were evaluated for safety.

Statistical analysis to detect a 6-month PFS of 35% was established based on data from previous studies [BRAIN study [24] (42.6% with bevacizumab monotherapy) and the NCI-06-C-0064E study [26] (29% with bevacizumab monotherapy)], in which a 15% threshold for 6-month PFS was defined. Under these conditions, 28 patients with recurrent GBM would provide at least 80% power to detect a 20% increase in 6-month PFS from 15 to 35% at the 5% one-sided significance level. Assuming that other WHO Grade III glioma patients would be enrolled, the overall target sample size was 32 patients.

The 6-month PFS, median PFS, OS and DOR were calculated by the Kaplan–Meier method and confidence intervals (CIs) calculated by Greenwood's formula (36). Exact binomial CIs were used for estimated intervals for response rates.

RESULTS

Patients

Between August 2009 and July 2010, 31 patients were enrolled, 29 of whom were included in the efficacy analysis population. All enrolled patients received a median of 6 bevacizumab doses. Treatment was discontinued in a total of 25 patients: 23 (74.2%) due to PD; 2 (6.5%) due to AEs. Efficacy and safety analyses, except for OS, were performed after an observation period of ≥6 months (data cut-off 7 January 2011); the OS analyses, which included data collected through to 22 August 2011, were performed after all enrolled patients had been observed for ≥1 year.

Demographic Data

The majority of patients (29; 93.5%) had GBM; 2 (6.5%) had Grade III glioma (Table 1). The median age was 54.0 years (range: 23–72); 10 (32.3%) patients were aged ≥65 years. The percentage of males to females was well balanced. Patients were in relatively good health with 61.3% having a KPS of 90–100, and 64.5% of patients not receiving corticosteroids at the start of the study. Similar numbers of patients had experienced 1 [17 (54.8%)] or 2 [14 (45.2%)] relapses.

Efficacy Outcomes

At the time the PFS and OS analyses were performed, 22 PD events and 21 death events had been reported in the 29 patients with recurrent GBM. The 6-month PFS rate in the 29 patients with recurrent GBM (primary endpoint) was 33.9% (90% CI, 19.2–48.5), and this exceeded the 15% threshold ($P = 0.0170$). Kaplan–Meier estimates of PFS showed a steady decline over the initial 6 months with a median PFS of 3.3 months (95% CI 2.8–6.0) (Fig. 1). The 1-year survival rate for these patients was 34.5% (90%

Table 1. Demographic and baseline disease characteristics

Parameter	All patients ($n = 31$)	GBM ($n = 29$)	WHO Grade III ($n = 2$)[a]
Median age, years (range)	54.0 (23–72)	57.0 (23–72)	32.5 (30–35)
Age groups in years, *n* (%)			
≤40	6 (19.4)	4 (13.8)	2 (100)
41–64	15 (48.4)	15 (51.7)	0 (0.0)
≥65	10 (32.3)	10 (34.5)	0 (0.0)
Gender, *n* (%)			
Male	16 (51.6)	14 (48.3)	2 (100)
Female	15 (48.4)	15 (51.7)	0 (0.0)
KPS, *n* (%)			
70–80	12 (38.7)	12 (41.4)	0 (0.0)
90–100	19 (61.3)	17 (58.6)	2 (100)
Relapse/progression status, *n* (%)			
First	17 (54.8)	17 (58.6)	0 (0.0)
Second	14 (45.2)	12 (41.4)	2 (100)
Duration of malignant glioma[b]			
Median, months (range)	15.2 (5.6–213.3)	15.0 (5.6–213.3)	46.8 (27.8–65.8)
Time from RT to bevacizumab[c]			
Median, months (range)	13.2 (3.8–209.6)	13.1 (3.8–209.6)	44.8 (25.5–64.1)
Corticosteroid use at baseline, *n* (%)			
Yes	11 (35.5)	10 (34.5)	1 (50.0)
No	20 (64.5)	19 (65.5)	1 (50.0)

GBM, glioblastoma; WHO, World Health Organization; KPS, Karnofsky performance status; RT, radiotherapy; q2w, every 2 weeks.
[a]One patient had anaplastic astrocytoma and one patient had anaplastic oligoastrocytoma.
[b]Time since the initial diagnosis of malignant glioma.
[c]Time from the last RT to the first dose of bevacizumab.

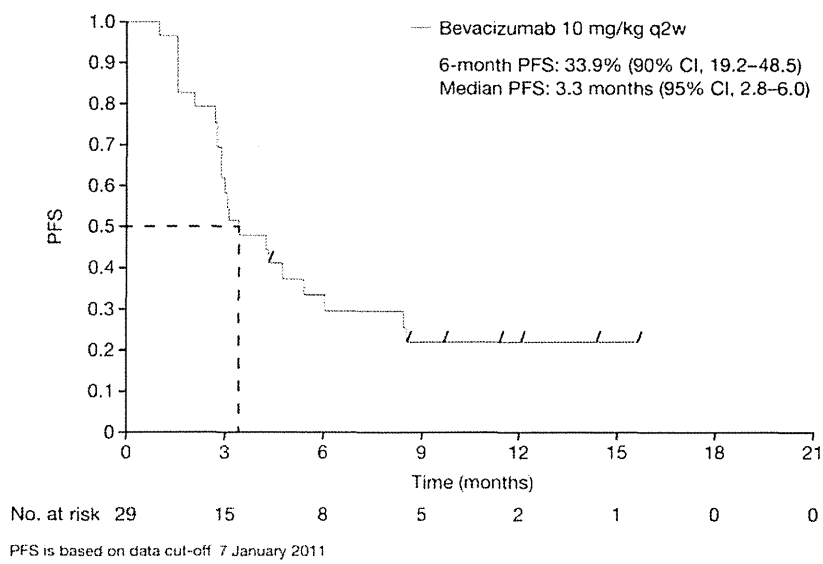

Figure 1. Progression-free survival determined by independent radiology facility in patients with recurrent glioblastoma (GBM).

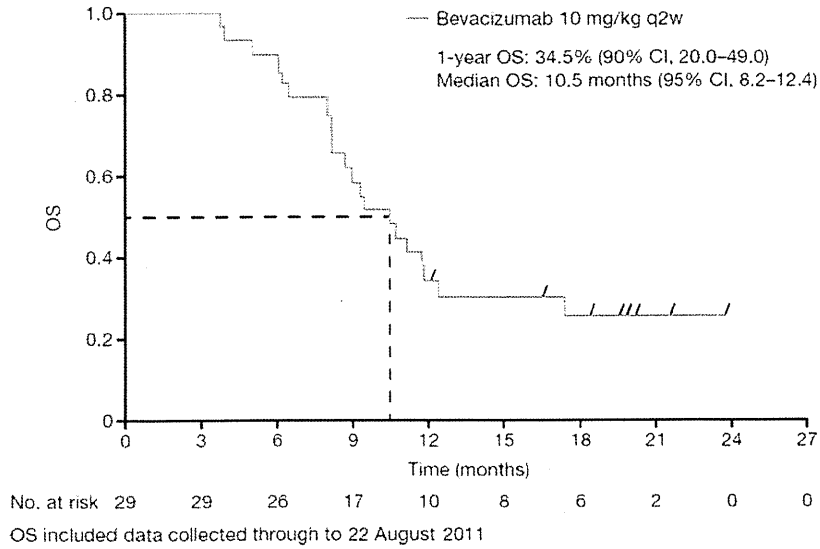

Figure 2. Overall survival in patients with recurrent GBM.

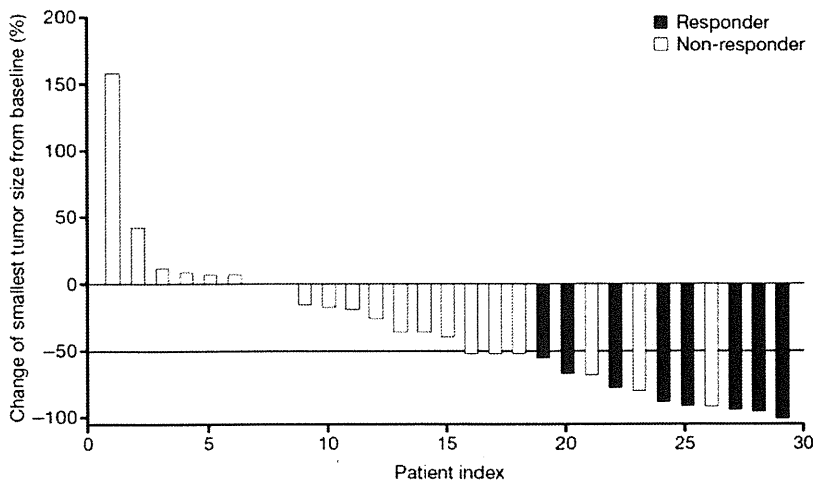

Figure 3. Waterfall plot showing the change in tumor size from baseline.

CI 20.0–49.0) with a median OS of 10.5 months (95% CI 8.2–12.4) (Fig. 2).

There were eight responders (all PR) with an ORR of 27.6% (95% CI 12.7–47.2). The DCR (0 CR + 8 PR + 15 NC) was 79.3% (95% CI 60.3–92.0). The two patients with WHO Grade III glioma completed one and two cycles of treatment, respectively; both experienced PD. Twenty-one patients (72.4%) with recurrent GBM experienced tumor shrinkage during the treatment period (Fig. 3), including 13 patients who were classified as non-responders. Of the 11 patients who were taking corticosteroids at baseline, dose reductions or discontinuation of corticosteroids occurred in 8 patients.

Efficacy endpoints were investigated in different patient subgroups (Table 2). Patients who were aged <50 years or <65 years, male, with a high KPS (90–100), on their first treatment relapse, not receiving corticosteroid therapy at baseline, or having been diagnosed with GBM at the initial diagnosis of malignant glioma, appeared to have a better response to bevacizumab treatment than other patients.

Safety Outcomes

All 31 patients experienced AEs with a total of 220 AEs reported during the study (Table 3). Serious AEs occurred in 11 (35.5%) patients, the most common being convulsion [2 (6.5%) patients]. Two (6.5%) patients discontinued the study due to AEs: one patient experienced a Grade 1 cerebral hemorrhage, and one patient had Grade 2 neutropenia that meant re-treatment within 6 weeks was not possible. A total of 13 (41.9%) patients experienced an AE of Grade ≥3, the most common being hypertension [3 (9.7%) patients]. No

Table 2. Six-month PFS and ORR by subgroup in patients with recurrent GBM

Variable	Bevacizumab 10 mg/kg, q2w ($n = 29$)	
	Six-month PFS, % (95% CI)	ORR, %
Age, years		
<65 ($n = 19$)	42.1 (19.9–64.3)	36.8
≥65 ($n = 10$)	15.0 (0.0–40.2)	10.0
Age, years		
<50 ($n = 11$)	45.5 (16.0–74.9)	45.5
≥50 ($n = 18$)	26.7 (5.7–47.6)	16.7
Gender		
Female ($n = 15$)	24.0 (1.3–46.7)	20.0
Male ($n = 14$)	42.9 (16.9–68.8)	35.7
KPS		
70–80 ($n = 12$)	16.7 (0.0–37.8)	8.3
90–100 ($n = 17$)	47.1 (23.3–70.8)	41.2
Relapse/progression status		
First ($n = 17$)	46.3 (22.3–70.4)	35.3
Second ($n = 12$)	16.7 (0.0–37.8)	16.7
Corticosteroid use at baseline		
Yes ($n = 10$)	20.0 (0.0–44.8)	10.0
No ($n = 19$)	42.1 (19.9–64.3)	36.8
Initial diagnosis of malignant glioma by site		
GBM ($n = 23$)	43.0 (22.6–63.5)	34.8
Other ($n = 6$)	0.0 (0.0–0.0)	0.0

PFS, progression-free survival; ORR, objective response rate; CI, confidence interval.

Table 3. Adverse events ≥Grade 3 and adverse events of special interest to bevacizumab

Patients, *n* (%)	Bevacizumab 10 mg/kg, q2w ($n = 31$)	
	All grade	Grade ≥3
Total patients with at least one AE	31 (100.0)	13 (41.9)
Irregular menstruation	3 (9.7)	2 (6.5)
Pyrexia	7 (22.6)	1 (3.2)
Convulsion	3 (9.7)	1 (3.2)
Depressed level of consciousness	1 (3.2)	1 (3.2)
Hydrocephalus	1 (3.2)	1 (3.2)
Increased intracranial pressure	1 (3.2)	1 (3.2)
Brain edema	1 (3.2)	1 (3.2)
Hemiplegia	1 (3.2)	1 (3.2)
Appendicitis	1 (3.2)	1 (3.2)
Urinary tract infection	1 (3.2)	1 (3.2)
Delirium	1 (3.2)	1 (3.2)
Neutropenia	5 (16.1)	1 (3.2)
Leukopenia	5 (16.1)	1 (3.2)
AEs of special interest to bevacizumab	22 (71.0)	5 (16.1)
Proteinuria	13 (41.9)	—
Hemorrhage[a,b]	10 (32.3)	—
Hypertension	10 (32.3)	3 (9.7)
Congestive heart failure	1 (3.2)	1 (3.2)
Venous thromboembolism	1 (3.2)	1 (3.2)

AE, adverse event.
[a]All events were Grade 1.
[b]Includes: epistaxis, gingival bleeding, conjunctival hemorrhage, infusion site hemorrhage, blood urine present, cerebral hemorrhage, hemorrhage subcutaneous, metrorrhagia.

incidence of Grade 4 or 5 hypertension was observed. One patient died of brain edema (Grade 5 AE), which was considered by the investigator to be related to PD with no causal relationship with bevacizumab treatment.

A total of 22 (71.0%) patients experienced AEs of special interest to bevacizumab, comprising proteinuria, hemorrhage, hypertension, congestive heart failure and venous thromboembolism (Table 3). One Grade 1 cerebral hemorrhage was observed on MRI; this was asymptomatic and resolved without treatment. Five (16.1%) patients had Grade 3 AEs of special interest to bevacizumab, comprising congestive heart failure [1 (3.2%) patient], venous thromboembolism [1 (3.2%) patient] and hypertension [3 (9.7%) patients]. No patients reported the other AEs of special interest to bevacizumab, i.e. reversible posterior leukoencephalopathy syndrome, wound-healing complications, GI perforation or fistulae.

Abnormal laboratory results were reported in 74.2% of patients. The most common abnormal laboratory result was proteinuria, which was reported in 41.9% of patients. Abnormal laboratory results classed as ≥Grade 3 were observed in two patients, reported as neutropenia and leukopenia.

DISCUSSION

This is the first clinical trial to investigate the safety and efficacy of single-agent bevacizumab in Japanese patients with recurrent GBM. Our data demonstrated that single-agent bevacizumab 10 mg/kg was effective in terms of the 6-month PFS, ORR, OS and 1-year survival, and was well tolerated in this Japanese population. In addition, the majority [21 (72.4%)] of patients with recurrent GBM experienced some tumor shrinkage during the treatment period.

The observed 6-month PFS of 33.9% and ORR of 27.6% seen in our study were more favorable than previous published data. These data are numerically higher than those reported for other studies with other chemotherapy and/or RT regimens (6-month PFS 9–21% and ORR 4–9%)

(6,7,10,11,37), and comparable with those reported for single-agent bevacizumab (42.6 and 28.2% for 6-month PFS and ORR, respectively) (24).

The use of Macdonald's Criteria was standard when this study was initiated; however, subsequently the Response Assessment in Neuro-Oncology (RANO) Working Group has recommended assessing MRI T2-weighted or fluid-attenuated inversion recovery (FLAIR) of non-enhancing lesions in addition to enhancing lesions (38). As the Macdonald's Criteria only assess contrast-enhancing lesions, there are risks that pseudoprogression and pseudoresponses may be considered real treatment effects. In our study an IRF assessed the changes in the T2/FLAIR signal, which was not included in the primary response evaluation based on Macdonald's Criteria. No significant increase in the T2/FLAIR signal was confirmed in the eight responders for the DOR, and seven out of eight responders exhibited $\geq$6 months' DOR. Based on these results, we are convinced that the objective response seen in our study is not a pseudoresponse.

Of the 29 GBM patients treated, 21 exhibited tumor shrinkage, including 8 patients who had a PR and 13 'non-responders' who were determined as NC or PD but exhibited some benefit with bevacizumab that was not captured by the response criteria; the maximum percentage of tumor shrinkage in 6 patients was >50%. The apparent discrepancy between the number of responders and the number of patients with tumor shrinkage is likely to be due to the ways in which the endpoints are calculated. The percentage of tumor shrinkage is calculated from the SPD at baseline and the smallest SPD after baseline, whereas for a patient to be classed as a responder, there had to be a decrease in tumor volume by $\geq$50% in the product of two diameters according to confirmation MRI performed $\geq$4 weeks after an observed response, as well as no increase in corticosteroid dosage and no neurologic deterioration. This leads to the difference between the number of patients with tumor shrinkage and the number of responders.

The 6-month PFS and ORR results were better for patients who had experienced one relapse than for those who had experienced two relapses, which is the same as a previously published observation (24). In addition, in our study bevacizumab improved the 6-month PFS and the ORR in the subgroups of patients who were aged <50 or <60 years compared with older patients. Although neither our study nor the previously published study (24) was powered to detect a statistical difference in these subgroups, the results could suggest that earlier administration of bevacizumab, or treatment with bevacizumab in younger patients, may lead to better tumor response and is something that requires investigation in further clinical trials.

Regarding the survival endpoints, our study showed results that were better than previously published data. The median OS of 10.5 months in GBM patients and 9.4 months in all patients was longer than that reported in other GBM trials (5.0–7.3 months) (6–8,10,11) and comparable with data with single-agent bevacizumab (9.3 months) (24,25). In addition, the 1-year survival rate for GBM patients (34.5%) was as good as the published data (14–32%) (6–8,10,11).

In addition to the favorable efficacy measures, a trend was also observed where 8 of the 11 patients who were taking corticosteroids at baseline were able to reduce their dose or discontinue corticosteroids altogether during the course of the study. This is consistent with other findings that suggest that bevacizumab may have corticosteroid-sparing effects in patients with recurrent GBM (39). Corticosteroid reduction may reduce infection rates and other related toxicities and therefore is expected to improve the health-related quality of life for patients.

Bevacizumab was well tolerated in our study and the incidence of AEs of special interest to bevacizumab was similar to that seen in other published studies with single-agent bevacizumab (24–26,40). No new bevacizumab safety signals were seen in this Japanese population.

In our study, and in the other single-agent bevacizumab studies (24–26,40), bevacizumab was administered after prior treatment with TMZ and RT. We observed an apparently greater benefit with bevacizumab in those patients with one relapse compared with those who have had two relapses following treatment with TMZ and RT. It is expected that bevacizumab may also provide benefit when administered concurrently with TMZ and RT rather than after TMZ/RT therapy. Currently, two randomized, double blind, Phase III studies are ongoing (AVAglio (41) and RTOG 0825 (42)) in which the addition of bevacizumab to standard of care (concurrent RT plus TMZ followed by adjuvant TMZ) is being evaluated in patients with newly diagnosed GBM.

There are many novel targeted agents under investigation for the treatment of gliomas (43); however, results with these new agents have been disappointing to date. Single-target agents alone may not be able to prevent tumor growth given the multiple pathways involved in many intracellular processes of tumor development. A key to future improvements in the treatment of gliomas will be the combination of other chemotherapeutic agents or molecular targeted therapies with bevacizumab to block these multiple pathways. This potential approach needs to be explored in future clinical trials.

In conclusion, the results of this study show that single-agent bevacizumab could provide significant clinical benefit for Japanese patients with recurrent GBM.

Acknowledgements

We are indebted to Dr Kazuhiro Nomura, Dr Shigeki Aoki and Tomoki Todo for their help in the assessment of efficacy and the evaluation of safety. We are also grateful to Dr Yoichi Nakazato for careful pathologic diagnosis.

Funding

This work was supported by Chugai Pharmaceutical Co. Ltd.

Conflict of interest statement

Dr Masao Matsutani is a coordinating investigator of this study, a member of the advisory committee on MSD KK and a member of the independent safety review board for Nobelpharma Co. Ltd; consulting fees as a coordinating investigator of this study have been received by him from Chugai Pharmaceutical Co. Ltd. Dr Ryo Nishikawa is a member of the Avaglio study steering committee (funded by F. Hoffmann-La Roche, Ltd) and has received research funding and speaking fees from MSD KK, and honoraria from Nobelpharma Co. Ltd. No other conflicts of interest were declared.

References

1. Hou LC, Veeravagu A, Hsu AR, Tse VC. Recurrent glioblastoma multiforme: a review of natural history and management options. *Neurosurg Focus* 2006;20:E5.
2. Ohgaki H. Epidemiology of brain tumors. *Methods Mol Biol* 2009;472:323–42.
3. Stupp R, Hegi ME, Mason WP, et al. Effects of radiotherapy with concomitant and adjuvant temozolomide versus radiotherapy alone on survival in glioblastoma in a randomised phase III study: 5-year analysis of the EORTC-NCIC trial. *Lancet Oncol* 2009;10: 459–66.
4. Stupp R, Mason WP, van den Bent MJ, et al. Radiotherapy plus concomitant and adjuvant temozolomide for glioblastoma. *N Engl J Med* 2005;352:987–96.
5. National Comprehensive Cancer Network. *NCCN Clinical Practice Guidelines in Oncology*. Central Nervous System Cancers V.2.2011. http://www.nccn.org/professionals/physician_gls/PDF/cns.pdf.
6. Lamborn KR, Yung WK, Chang SM, et al. Progression-free survival: an important end point in evaluating therapy for recurrent high-grade gliomas. *Neuro Oncol* 2008;10:162–70.
7. Ballman KV, Buckner JC, Brown PD, et al. The relationship between six-month progression-free survival and 12-month overall survival end points for phase II trials in patients with glioblastoma multiforme. *Neuro Oncol* 2007;9:29–38.
8. van den Bent MJ, Brandes AA, Rampling R, et al. Randomized phase II trial of erlotinib versus temozolomide or carmustine in recurrent glioblastoma: EORTC brain tumor group study 26034. *J Clin Oncol* 2009;27:1268–74.
9. Wong ET, Hess KR, Gleason MJ, et al. Outcomes and prognostic factors in recurrent glioma patients enrolled onto phase II clinical trials. *J Clin Oncol* 1999;17:2572–8.
10. Wick W, Puduvalli VK, Chamberlain MC, et al. Phase III study of enzastaurin compared with lomustine in the treatment of recurrent intracranial glioblastoma. *J Clin Oncol* 2010;28:1168–74.
11. Yung WK, Albright RE, Olson J, et al. A phase II study of temozolomide vs. procarbazine in patients with glioblastoma multiforme at first relapse. *Br J Cancer* 2000;83:588–93.
12. Huang H, Held-Feindt J, Buhl R, Mehdorn HM, Mentlein R. Expression of VEGF and its receptors in different brain tumors. *Neurol Res* 2005;27:371–7.
13. Chaudhry IH, O'Donovan DG, Brenchley PE, Reid H, Roberts IS. Vascular endothelial growth factor expression correlates with tumor grade and vascularity in gliomas. *Histopathology* 2001;39: 409–15.
14. Fukumura D, Xu L, Chen Y, Gohongi T, Seed B, Jain RK. Hypoxia and acidosis independently up-regulate vascular endothelial growth factor transcription in brain tumors *in vivo*. *Cancer Res* 2001;61: 6020–4.
15. Stefanik DF, Fellows WK, Rizkalla LR, et al. Monoclonal antibodies to vascular endothelial growth factor (VEGF) and the VEGF receptor, FLT-1, inhibit the growth of C6 glioma in a mouse xenograft. *J Neurooncol* 2001;55:91–100.
16. Hurwitz H, Fehrenbacher L, Novotny W, et al. Bevacizumab plus irinotecan, fluorouracil and leucovorin for metastatic colorectal cancer. *N Engl J Med* 2004;350:2335–42.
17. Johnson DH, Fehrenbacher L, Novotny W, et al. Randomised Phase II trial comparing bevacizumab plus carboplatin and paclitaxel with carboplatin and paclitaxel alone in previously untreated locally advanced or metastatic non-small-cell-lung cancer. *J Clin Oncol* 2004;22:2184–91.
18. Miller K, Wang M, Gralow J, et al. Paclitaxel plus bevacizumab versus paclitaxel alone for metastatic breast cancer. *N Engl J Med* 2007; 357:2666–76.
19. Yang JC, Haworth L, Sherry RM, et al. A randomised trial of bevacizumab, and anti-vascular endothelial growth factor antibody, for metastatic renal cancer. *N Engl J Med* 2003;349:427–34.
20. *How Avastin is Designed to Work [Internet]*. USA: Genentech, 2012 (cited 23 March 2012). http://www.avastin.com/avastin/patient/gbm/index.html.
21. *FDA Approves Drug for Treatment of Aggressive Brain Cancer [Internet]*. MD, USA: Food and Drug Administration, 2009 (cited 12 January 2012). www.fda.gov/NewsEvents/Newsroom/PressAnnouncements/2009/ucm152295.htm.
22. Stark-Vance V. Bevacizumab and CPT-11 in the treatment of relapsed malignant glioma. *Neuro-Oncol* 2005;7:369. Abstract 342.
23. Vrendenburgh JJ, Desjardins A, Herndon JE, II, et al. Bevacizumab plus irinotecan in recurrent glioblastoma multiforme. *J Clin Oncol* 2007;25:4722–9.
24. Friedman HS, Prados MD, Wen PY, et al. Bevacizumab alone and in combination with irinotecan in recurrent glioblastoma. *J Clin Oncol* 2009;27:4733–40.
25. Cloughesy T, Vredenburgh JJ, Day B, Das A, Friedman HS. Updated safety and survival of patients with relapsed glioblastoma treated with bevacizumab in the BRAIN study. *J Clin Oncol* 2010;28(Suppl):181s. Abstract 2008.
26. Kreisl TN, Kim L, Moore K, et al. Phase II trial of single-agent bevacizumab followed by bevacizumab plus irinotecan at tumor progression in recurrent glioblastoma. *J Clin Oncol* 2009; 27:740–5.
27. Raizer JJ, Grimm S, Chamberlain MC, et al. Phase 2 trial of single-agent bevacizumab given in an every-3-week schedule for patients with recurrent high-grade gliomas. *Cancer* 2010;116:5297–305.
28. Kairouz VF, Elias EF, Chahine GY, Comair YG, Dimassi H, Kamar FG. Final results of an extended phase II trial of bevacizumab and irinotecan in relapsed high grade gliomas. *Neuro-Oncol* 2010;12(Suppl 4):iv40–1. Abstract NO-20.
29. Gil MJ, de las Peñas R, Reynés G, et al. Bevacizumab plus irinotecan in recurrent malignant glioma showed high overall survival in a retrospective study. *Neuro-Oncol* 2010;12(Suppl. 4):iv53. Abstract NO-73.
30. Nghiemphu PL, Liu W, Lee Y, et al. Bevacizumab and chemotherapy for recurrent glioblastoma: a single-institution experience. *Neurology* 2009;72:1217–22.
31. Sathornsumetee S, Desjardins A, Vredenburgh JJ, et al. Phase II trial of bevacizumab and erlotinib in patients with recurrent malignant glioma. *Neuro-Oncol* 2010;12:1300–10.
32. Francesconi AB, Dupre S, Matos M, et al. Carboplatin and etoposide combined with bevacizumab for the treatment of recurrent glioblastoma multiforme. *J Clin Neurosci* 2010;17:970–4.
33. Soffietti R, Trevisan E, Ruda R, et al. Phase II trial of bevacizumab with fotemustine in recurrent glioblastoma: final results of a multicenter study of AINO (Italian Association of Neuro-oncology). *J Clin Oncol* 2011;29(Suppl):146. Abstract 2027.
34. Macdonald DR, Cascino TL, Schold SC, Cairncross JG. Response criteria for phase II studies of supratentorial malignant glioma. *J Clin Oncol* 1990;8:1277–80.
35. Trotti A, Colevas AD, Setser A, et al. CTCAE v3.0: development of a comprehensive grading system for the adverse effects of cancer treatment. *Semin Radiat Oncol* 2003;13:176–81.
36. Greenwood M. Reports on public health and medical subjects. The Error of Sampling of the Survivorship Tables. No 33, Appendix 1, London, UK: H.M Stationary Office, 1926.
37. Happold C, Roth P, Wick W, et al. ACNU-based chemotherapy for recurrent glioma in the temozolomide era. *J Neurooncol* 2009; 92:45–8.

38. Wen PY, Macdonald DR, Reardon DA, et al. Update response assessment criteria for high-grade gliomas: Response Assessment in Neuro-Oncology Working Group. *J Clin Oncol* 2010;28:1963–72.
39. Vredenburgh JJ, Cloughesy T, Samantc M, et al. Corticosteroid use in patients with glioblastoma at first or second relapse treated with bevacizumab in the BRAIN study. *Oncologist* 2010;15:1329–34.
40. Chamberlain MC, Johnston SK. Salvage therapy with single-agent bevacizumab for recurrent glioblastoma. *J Neurooncol* 2010;96:259–69.
41. *A Study of Avastin (bevacizumab) in Combination with Temozolomide and Radiotherapy in Patients with Newly Diagnosed Glioblastoma [Internet]*. USA: Clinicaltrials.gov, 2009 (cited 4 October 2011). http://clinicaltrials.gov/ct2/show/NCT00943826.
42. *Temozolomide and Radiation Therapy with or Without Bevacizumab in Treating Patients with Newly Diagnosed Glioblastoma [Internet]*. USA: Clinicaltrials.gov, 2009 (cited 4 October 2011). http://clinicaltrials.gov/ct2/show/NCT00884741.
43. Van Meir EG, Hadjipanayis CG, Norden AD, et al. Exciting new advances in neuro-oncology: the avenue to a cure for malignant glioma. *CA Cancer J Clin* 2010;60:166–93.

Int J Clin Oncol
DOI 10.1007/s10147-013-0517-x

ORIGINAL ARTICLE

Predictive significance of mean apparent diffusion coefficient value for responsiveness of temozolomide-refractory malignant glioma to bevacizumab: preliminary report

Motoo Nagane · Keiichi Kobayashi · Masaki Tanaka · Kazuhiro Tsuchiya · Yukiko Shishido-Hara · Saki Shimizu · Yoshiaki Shiokawa

Received: 24 September 2012 / Accepted: 25 December 2012

Abstract
Background Recurrent glioblastoma after initial radiotherapy plus concomitant and adjuvant temozolomide is problematic. Here, patients with temozolomide-refractory high-grade gliomas were treated with bevacizumab (BV) and evaluated using apparent diffusion coefficient (ADC) for response.
Methods Nine post-temozolomide recurrent or progressive high-grade glioma patients (seven with glioblastoma and two with anaplastic astrocytoma) were treated with BV monotherapy. Average age was 57 years (range, 22–78), median Karnofsky Performance Scale (KPS) was 70 (30–80) and median BV line number was 2 (2–5). Two had additional stereotactic radiotherapy within 6 months prior to BV. Magnetic resonance (MR) imaging after BV therapy was performed within 2 weeks with calculation of mean ADC (mADC) values of enhancing tumor contours.
Results Post-BV treatment MR imaging showed decreased tumor volumes in eight of nine cases (88.9 %). Partial response was obtained in four cases (44.4 %), four cases had stable disease, and one had progressive disease. Of 15 evaluable enhancing lesions, 11 shrank and four did not. Pretreatment mADC values were above 1100 (10^{-6} mm^2/s) in all responding tumors, while all non-responding lesions scored below 1100 ($p = 0.001$). mADC decreased after the first BV treatment in all lesions except one. KPS improved in four cases (44.4 %). Median progression-free survival and overall survival for those having all lesions with high mADC (>1100) were significantly longer than those with a low mADC (<1100) lesion ($p = 0.018$ and 0.046, respectively).
Conclusions Bevacizumab monotherapy is effective in patients with temozolomide-refractory recurrent gliomas and tumor mean ADC value can be a useful marker for prediction of BV response and survival.

Keywords Glioblastoma · Bevacizumab · Apparent diffusion coefficient · Prediction of response and survival · Recurrent high-grade glioma

Introduction

Standard care for glioblastoma (GBM) is radiation therapy (RT) plus concomitant and adjuvant temozolomide (TMZ) [1]. The median overall survival (OS) of patients with GBM remains at 15 months from initial diagnosis [1], and there are no standard therapies established for recurrent GBMs.

These data were previously presented at the 2011 Annual Meeting of American Society of Clinical Oncology (ASCO), Chicago, USA, 4 June 2011, and the 16th Annual Meeting of the Society for Neuro-Oncology (SNO), Anaheim, USA, 18–21 November 2011.

M. Nagane (✉) · K. Kobayashi · M. Tanaka · S. Shimizu · Y. Shiokawa
Department of Neurosurgery, Kyorin University Faculty of Medicine, 6-20-2 Shinkawa, Mitaka, Tokyo 181-8611, Japan
e-mail: mnagane.g@gmail.com

K. Tsuchiya
Department of Radiology, Kyorin University Faculty of Medicine, 6-20-2 Shinkawa, Mitaka, Tokyo 181-8611, Japan

Y. Shishido-Hara
Department of Pathology, Kyorin University Faculty of Medicine, 6-20-2 Shinkawa, Mitaka, Tokyo 181-8611, Japan

Published online: 26 January 2013

Glioblastoma is highly vascularized and vascular endothelial growth factor (VEGF) has been identified as the major promoting factor for glioma angiogenesis [2]. VEGF expression correlates with aggressiveness and histopathological grade of glioma [3]. VEGF induces an increase in vascular permeability and disruption of the blood–brain barrier (BBB) in tumors. High-grade gliomas with abundant VEGF expression exhibit an increase in interstitial fluids, causing peri- and intra-tumoral edema [4], and further neurological deterioration. It would, therefore, be reasonable to target VEGF as a potential therapeutic strategy against intractable GBM [5].

Bevacizumab (BV) is a humanized monoclonal antibody that binds to and inhibits the activity of VEGF. The efficacy of BV for recurrent GBM was demonstrated in initial phase II clinical trials in combination with irinotecan [6]. BV monotherapy for patients with TMZ-pretreated, recurrent GBM achieved progression-free survival (PFS) at 6 months (PFS-6 m) of 43 % and median OS of 9.3 months [7]. This and another similar phase II study [8] led to accelerated approval for use of BV as a single-agent in adults with recurrent GBM in the United States. However, a subset of GBM lesions do not respond to BV, and this necessitates a way to differentiate tumors that will respond from those that will not, given the adverse effects of BV such as intracerebral hemorrhage and deep venous thrombosis, and also the high cost of the agent.

Bevacizumab decreases interstitial fluid load in the brain and tumor tissue by normalizing the BBB, leading to rapid tumor shrinkage with reduction of perifocal edema [5, 7]. An imaging technique that specifically detects such pathological conditions would be useful for prediction of BV response. One physiological imaging biomarker that might be associated with degradation of cellular integrity, such as necrosis, is apparent diffusion coefficient (ADC) obtained on diffusion-weighted magnetic resonance (MR) imaging. The ADC value represents movement of water molecules and tends to be low in tissues with high cellular density (packed tumor) where extracellular space is restricted [9]. Conversely, tissue edema and necrotic components induced by tumor burden and cytotoxic therapies may well increase the ADC value [10, 11]. The ADC value has been shown to correlate with response to radiation therapy (RT) and prognosis in patients with glioma [12, 13], to predict progression-free survival (PFS) after BV treatment in patients with recurrent GBM, and the minimum ADC values were reportedly prognostic of outcomes in glioma [12, 14]. This prompted us to investigate whether the ADC value in recurrent high-grade glioma may predict rapid shrinking response or survival after BV monotherapy, thereby facilitating selection of patients who are likely responders.

Patients and methods

Patient eligibility

Patients (≥20 years old) had histologically proven high-grade glioma (HGG) for which they had received RT and TMZ. All had experienced tumor progression determined by the Macdonald criteria [15], had measurable enhancing disease(s) on MR imaging, and had recovered from their prior treatment. The minimum 4 weeks from surgical therapy and 8 weeks after RT must have elapsed before the start of BV treatment. The patients had to have adequate organ functions and were excluded if they had experienced cerebral hemorrhage or stroke. Patients were required to have provided written informed consent. The treatment protocol including off-label use of BV at patients' own cost was reviewed and approved by the institutional review board.

Treatment

All patients received BV 10 mg/kg intravenously every other week, until disease progression or discontinuation by their withdrawal, grade 2 or more cerebral hemorrhage, grade 4 non-hematological toxicities, or any other condition that would make the treatment unsafe.

Patient evaluation

The response to therapy was assessed using MR imaging and neurological examination. The Macdonald criteria were employed to evaluate the MR imaging [15]. The criteria use the largest cross-sectional area of the post-contrast T1-weighted images and also take into account the steroid dose and clinical findings. We also evaluated non-contrast T1-weighted images, T2-weighted images, FLAIR images, and diffusion-weighted images. All MR examinations were carried out at 1.5 T. MR imaging was performed after the first and the third cycles of BV treatment, and images were reviewed by a neuroradiologist (K.T.).

Measurement of mean apparent diffusion coefficient ADC value of tumors

A mean ADC (mADC) value of the tumor was calculated on a terminal of the Picture Archiving and Communication System (PACS). Gadolinium-enhancing tumor contours were manually segmented on sequential post-contrast T1-weighted images, eliminating non-enhancing regions within the tumor, and the same segmented areas were selected on the corresponding ADC maps, thereby obtaining a mADC value (10^{-6}mm^2/s) and an area (mm^2) of the tumor in each image (Fig. 1). The mADC value of the image slice was multiplied by the area to produce a total ADC value of

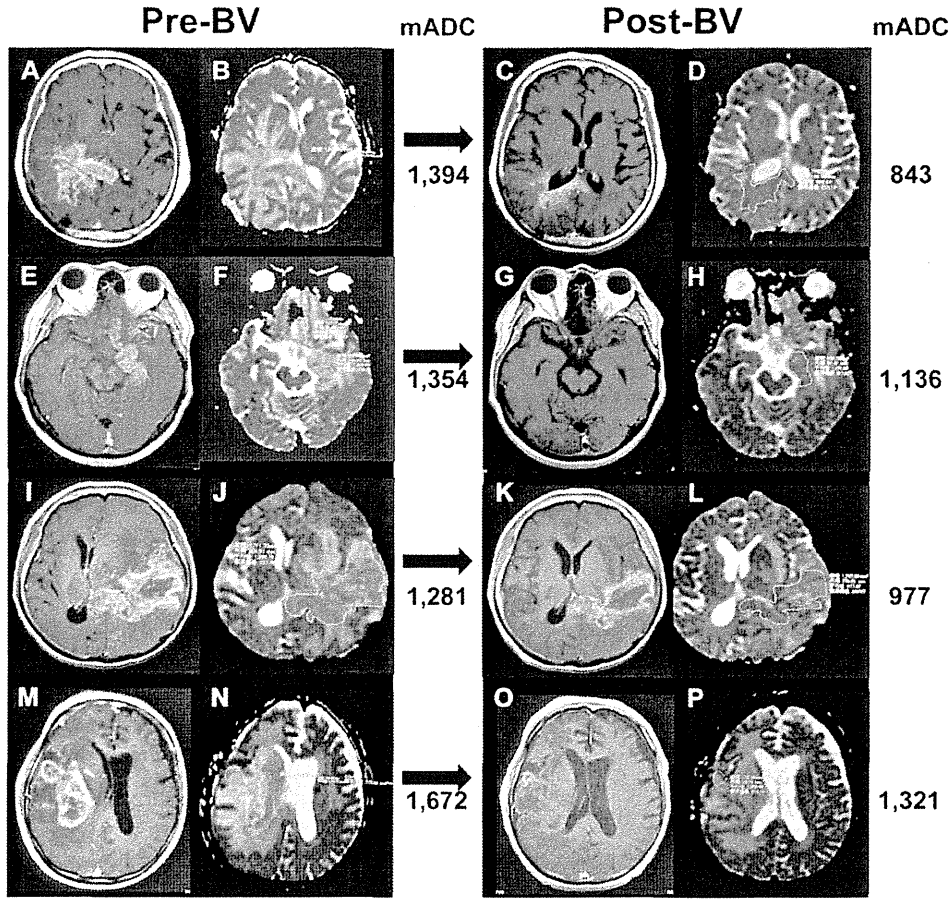

Fig. 1 Postcontrast T1-weighted images aligned side-by-side with the corresponding ADC maps of both pre- (*left-hand column*) and post-treatment (*right-hand column*) with BV in representative patients who achieved immediate response after a single BV administration. The mADC values of the lesions of interest are indicated at the *right margin* of the ADC maps. Each mADC value is calculated as described in "Patients and methods." Note that all pretreatment mADC values are above 1100 (10^{-6} mm^2/s), which subsequently decrease after BV treatment. **a, b, c, d**: case 1; **e, f, g, h**: case 2; **i, j, k, l**: case 8; **m, n, o, p**: case 9

the slice. The sum of the total ADC value of all slices for a lesion was divided by the sum of areas of all slices to achieve the net mADC value of the single enhancing lesion.

Immunohistochemistry

Immunohistochemistry analysis of surgical specimens of the original tumors entailed: (1) fixation with 10 % buffered formalin, and embedding in paraffin; (2) deparaffinizing 5-μm-thick sections of the tissues in xylene, and rehydration in 90, 70, and 50 % ethanol; (3) antigen retrieval, by autoclaving in buffered citrate (pH 7.0) at 120 °C for 10 min; (4) incubation with the primary antibody, anti-VEGF antibody (code SC-152, Santa Cruz, CA, USA) at room temperature for approximately 12 h; and (5) detection of immunoreactivity using the EnVision system (Dako, Carpinteria, CA, USA), followed by hematoxylin counterstaining.

O^6-methylguanine-DNA methyltransferase (*MGMT*) status

Methylation status of the *MGMT* gene promoter region in tumors was determined by the methylation-specific polymerase chain reaction as described elsewhere [16].

Statistical analysis

The correlation of the mADC value with response to BV was evaluated by Fisher's exact test and the Mann–Whitney *U* test. The change of mADC values before and after the first BV treatment was assessed by a paired *t* test. PFS and OS were calculated according to the Kaplan–Meier method, and differences in progression and survival according to mADC values were evaluated with the log-rank test. All the probability values were two-sided, and all statistical analyses were done at a significance level of $p = 0.05$, using the statistical package SPSS 17.0J (SPSS, Inc., Chicago, IL, USA).

Results

Bevacizumab treatment of patients with recurrent HGG after TMZ failure

From August 2009 to December 2010, nine eligible patients with recurrent or progressive HGGs (seven with GBM and two with anaplastic astrocytoma) were treated with BV monotherapy. The average patient age was 57